RESEARCH PAPERS

Comparison of methods for determining orthotropic axes in 3D femur remodeling*

Shang Yu, Bai Jing**, Peng Liang and Lau Jaclyn

(Department of Biomedical Engineering, Tsinghua University, Beijing 100084, China)

Accepted on August 7, 2007

Abstract The density distribution and internal structure of trabecular bone are modulated by local mechanical environment. In this study, an orthotropic adaptation algorithm was applied to the 3D femur model to simulate the variations of stiffness and orientation of trabecular bone under multi-loading conditions. This algorithm includes the determination of orthotropic axes and the stiffness modification of trabecular bone. Three methods were used to determine the orthotropic axes, i. e. the maximal cycle method, the stress maximum method, and the composite method. We found that the composite method was better than the other two. Firstly, the characteristics of density distribution obtained by using the composite method agreed better with those in real proximal femur. Secondly, the material orientation aligned with the known trabeculaer pattern. Finally, the ratios of the longitudinal modulus to the transverse modulus were also shown to be realistic in three local regions of the proximal femur.

Keywords: orthotropic axes, trabecular bone, adaptation algorithm, stiffness variation.

Many studies have shown that the density distribution and internal structure of trabecular bone are modulated by local mechanical environment[1—3]. The osteocytes sense the mechanical stimuli and respond to them by activating the osteoblasts and osteoclasts, which may result in bone formation or resorption. It is important to estimate the variations of bone structure and strength under the altering load condition, especially for the people in a certain environment such as the astronauts in the space and the long-term bed-rest patients, since their bone structures may change and adapt to new mechanical environment.

The relationship between bone structure and mechanical stimulus is assumed to conform to a certain mathematical law[4], though the exact adaptive mechanism is largely unknown[5]. A lot of adaptation algorithms have been proposed. They may be classified as either error driven or non-error driven algorithm[6]. The mechanical stimulus is adjusted towards the equilibrium value in error driven algorithm. In most adaptation algorithms, the trabecular bone is assumed to be isotropic, and the stress, strain or strain energy density is used as mechanical stimulus[1,7—9]. With the isotropic algorithm, the trabeculae can be displayed in the small-scale bone specimen[10], but the orientation characteristic of trabecular bone can be hardly described in the scale as large as the whole femur. In addition, trabecular bone is anisotropic rather than isotropic[11—13]. The Young's modulus in the vertical direction is almost twice that in the horizontal direction[14], since the loads in the vertical direction are dominant for normal people during their daily activities. There exist several adaptation algorithms that take orthotropy or anisotropy into consideration[15—18]. Miller et al. proposed a novel orthotropic adaptation algorithm[17], in which the Young's moduli of trabecular bone varied in the principal stress directions so that the trabecular pattern could be displayed. They had used this algorithm to simulate the remodeling process of the trabecular bone in two-dimensional (2D) proximal femur, and the orthotropic axes of each trabecular element were determined by single load case.

The multiple load cases have positive significance in bone adaptation for realistic consideration. Moreover, the orientation characteristic of three-dimensional (3D) trabecular bone is useful for the research

* Supported by National Natural Science Foundation of China (Grant No. 60571013), the Tsinghua-Yue-Yuen Medical Science Foundation, the National Basic Research Program of China (Grant No. 2006CB705701), and the Special Research Fund for the Doctoral Program of Higher Education of China (Grant No. 20050003090)

** To whom correspondence should be addressed. E-mail: deabj@tsinghua.edu.cn

on the internal bone structure, especially for practical application. In this study, an orthotropic adaptation algorithm was applied to a 3D femur for the purpose of simulating the variations of stiffness, density and internal structure of trabecular bone under multi-loading conditions. Three methods for determining the orthotropic axes, i.e. the maximal cycle method, the stress maximum method, and the composite method, were used and compared. The load case with maximal cycles was adopted in the maximal cycle method. Whereas the load case with the maximum of all the principal stresses was adopted in the stress maximum method. This method was initiated by Miller et al.[17]. The composite method considers both the loading cycles and the principal stress with different weighting factors, and the orthotropic axes are determined by multiple load cases. The Young's moduli of trabecular bone change according to a certain error driven algorithm in which a strain based variable is defined and chosen as the mechanical stimulus.

The numerical solutions were obtained by combining the adaptation algorithm with the finite element (FE) method. The FE model was established based on the 3D CT data set of real femur. The stiffness, density and material orientation were calculated to compare the three determination methods quantitatively.

1 Methods

1.1 FEA model

A 3D geometrical model was reconstructed from the male CT data set obtained from the visible human project (VHP) of the National Library of Medicine (NLM, USA), and then it was transferred to the commercial FE software MARC 2003 (MSC, USA). The model was meshed with eight-node hexahedron element. The number of elements and nodes was 24441 and 29161, respectively[19]. The whole femur was assumed to be made up of two parts with its exterior shell consisting of dense cortical bone, and the internal part consisting of porous trabecular bone. Cortical bone is nearly transversely isotropic and was supposed to remain constant during the adaptive process. The Young's modulus, shear modulus and Poisson's ratio of the cortical bone in the longitudinal direction were $E_L=16.61$ Gpa, $G_L=4.74$ Gpa, and $\nu_L=0.370$, respectively. As for the transverse direction, $E_T=9.55$ Gpa, $G_T=3.28$ Gpa and $\nu_T=0.45$, respectively[20].

The trabecular bone of the femur was assumed to be uniform and isotropic with $E=423$ Mpa and $\nu=0.3$ in the original state. The distal femur was firmly constrained in all directions. Three load cases were applied to the femur head and the greater trochanter respectively (Fig. 1). The magnitude and the direction of each force as well as the cycles of each load case were the same as those adopted by Doblaré et al.[16]. We assumed that the trabecular bone remained orthotropic after the first iteration, though the stiffness and the three symmetry planes of each element varied in different iterative steps.

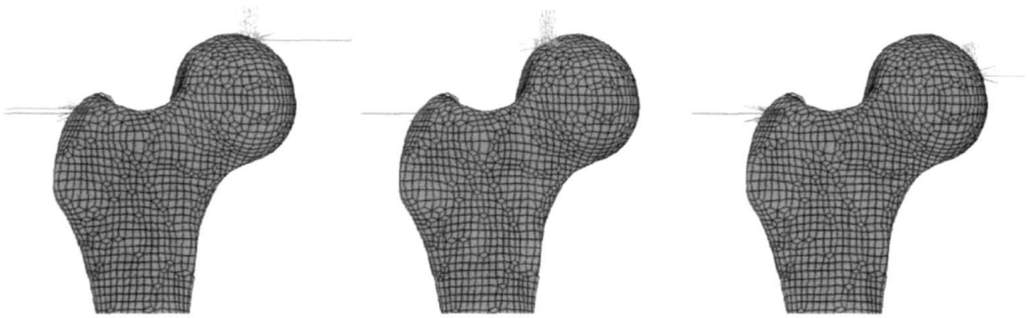

Fig. 1. Three load cases on the proximal femur. They are shown from left to right respectively. Every load case includes joint reaction force on femoral head and abductor force on greater trochanter, which is the same as that adopted by Doblaré et al.[16]. Each force is distributed uniformly among five adjacent nodes.

1.2 Adaptation algorithm

The adaptation algorithm includes two steps: determination of the orthotropic axes and stiffness modification of the trabecular bone. Three determination methods, maximal cycle method, stress maximum method, and composite method, were used in this study.

The maximal cycle method means that the or-

thotropic axes are determined by the load case with maximal cycles. In this study, the cycles of the first load case was larger than that of the two other load cases. Therefore, the principal stress directions of every element under the first load case were calculated and chosen as local material axes.

The stress maximum method had been adopted by Miller et al. in the 2D model[17], where only two material axes were needed to be determined. We developed this method for 3D application in our study. Three principal stresses of each trabecular element under each load case were calculated. Then, they were rearranged according to their magnitudes. For the ith element under the jth load case, this arrangement can be denoted as the following inequality:

$$|\sigma_{1(i,j)}| \geqslant |\sigma_{2(i,j)}| \geqslant |\sigma_{3(i,j)}| \quad (1)$$

Then, the load case J was chosen to satisfy the equation

$$|\sigma_{1(i,J)}| = \max_{1\leqslant j\leqslant 3}(|\sigma_{1(i,j)}|) \quad (2)$$

Finally, the three principal stress directions under the load case J were chosen as local material axes for the ith element.

The composite method is a composition of the maximal cycle method and the stress maximum method. Three local material axes are determined step by step. Firstly, three principal stresses of each trabecular element under each load case were rearranged according to their magnitudes. This is the same as that mentioned in the stress maximum method. The direction of the kth axis in the ith element under the jth load case was denoted as a unit vector $\boldsymbol{g}_{k(i,j)}$. Due to the largest cycles of the first load case, let $\boldsymbol{g}_{1(i,j)}$ be the negative vector if $\boldsymbol{g}_{1(i,1)} \cdot \boldsymbol{g}_{1(i,j)} < 0$ $(j = 2, 3)$. Thus, the vectors determined by other load cases will not form an obtuse angle with $\boldsymbol{g}_{1(i,1)}$. Secondly, the new vector was defined as:

$$\boldsymbol{f}_{k(i,j)} = (n_j)^{1/m} |\sigma_{k(i,j)}| \boldsymbol{g}_{k(i,j)} \quad (k = 1, 2, 3) \quad (3)$$

where m is an empirical constant (larger m value means that the principal stress is weighted more heavily than the loading cycles), and n_j is the cycles of the jth load case per day. The first direction of the local material axes was determined by the formula

$$\boldsymbol{e}_{1(i)} = \frac{\sum_j \boldsymbol{f}_{1(i,j)}}{\left|\sum_j \boldsymbol{f}_{1(i,j)}\right|} \quad (4)$$

Thirdly, we calculated the projection of $\boldsymbol{f}_{2(i,j)}$ in the plane vertical to $\boldsymbol{e}_{1(i)}$, that is

$$\boldsymbol{pf}_{2(i,j)} = \boldsymbol{f}_{2(i,j)} - (\boldsymbol{f}_{2(i,j)} \cdot \boldsymbol{e}_{1(i)})\boldsymbol{e}_{1(i)} \quad (5)$$

Similarly, if $\boldsymbol{pf}_{2(i,1)} \cdot \boldsymbol{pf}_{2(i,j)} < 0$ $(j = 2, 3)$, let $\boldsymbol{pf}_{2(i,j)}$ be the negative vector. Finally, the second direction is determined by

$$\boldsymbol{e}_{2(i)} = \frac{\sum_j \boldsymbol{pf}_{2(i,j)}}{\left|\sum_j \boldsymbol{pf}_{2(i,j)}\right|} \quad (6)$$

The third direction is

$$\boldsymbol{e}_{3(i)} = \boldsymbol{e}_{1(i)} \times \boldsymbol{e}_{2(i)} \quad (7)$$

Thus, the local material axes were determined and every two axes of them were vertical to each other.

The Young's moduli of trabecular bone change along the local material axes and their variation ratios are given by the following error driven algorithm[17]:

$$\frac{dE_{k(i)}}{dt} = \begin{cases} B[\Psi_{k(i)} - \Psi_0(1+s)] & \text{if } \Psi_{k(i)} \geqslant \Psi_0(1+s) \\ 0 & \text{if } \Psi_0(1-s) < \Psi_{k(i)} < \Psi_0(1+s) \\ B[\Psi_{k(i)} - \Psi_0(1-s)] & \text{if } \Psi_{k(i)} \leqslant \Psi_0(1-s) \end{cases} \quad (8)$$

where $E_{k(i)}$ $(k = 1, 2, 3;\ i = 1, 2, \cdots, 24441)$ represents the Young's modulus in the k direction of the ith element, B is a constant, Ψ_0 is the equilibrium value, and it is also a constant. The mechanical stimulus $\Psi_{k(i)}$ is

$$\Psi_{k(i)} = \frac{1}{E_{k(i)}}\left(\sum_j n_j |\sigma^m_{k(i,j)}|\right)^{1/m} \quad (9)$$

where m and n_j have the same meaning as those mentioned above. The weighted sum of principal stresses divided by Young's modulus means that the mechanical stimulus is a strain based variable. The idea of "lazy zone"[8] was employed in this algorithm, and s is the parameter regulating the width of the lazy zone. The shear moduli also change according to the formula:

$$G_{ij} = \frac{E_i + E_j}{4(1+\nu)}, \quad (ij = 12, 23, 31) \quad (10)$$

Each of the ν_{12}, ν_{13}, ν_{23} is equal to ν all the time since little evidence has been found in the relationship between the Poisson's ratio and the moduli[21]. Due to the thermodynamic restriction[18], let $E_i = E_j\nu_{ij}$ $(ij = 12, 23, 31)$ if $E_i < E_j\nu_{ij}$. Hence, $E_i \geqslant E_j\nu_{ij} > E_j\nu_{ij}^2$, and the compliance matrix in the FE analysis is sure to be definitely positive. The maximum and minimum of Young's moduli were set as 1320 Mpa and 44 Mpa. If the Young's moduli of over 95% of

trabecular elements remain the same, the iteration will stop and this means that the steady structure of femur is attained.

The iteration process of bone remodeling is shown in Fig. 2. Each iteration step includes the FE calculation and the updating of the principal axes and stiffness by the adaptation algorithm.

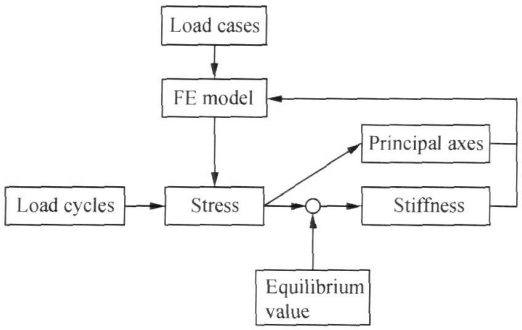

Fig. 2. The flow chart of the trabecular bone remodeling. Each iteration step includes FE calculation and updating of the principal axes and stiffness by the adaptation algorithm.

1.3 Evaluation

The most important criterions for comparing the three determination methods are the distributions of bone density and trabecular alignment, since their general patterns among different individuals are similar[22]. In addition, the results were also evaluated in terms of the ratio of the longitudinal modulus to the transverse modulus (L-T ratio). Bone density can be acquired through the formula $E = 1904\rho^{1.64}$ [14], where E is the average of Young's moduli in three material directions. The moduli in x, y, z directions can be derived from the stiffness matrix in the FE analysis. The L-T ratio is defined as $2E_{zz}/(E_{xx}+E_{yy})$. The projection of material axis in the coronal section is used to describe the trabecular alignment in the 2D plane.

2 Results

To evaluate the validity of the three methods objectively, the parameters adopted in this simulation have been made to be the same for all the methods. All the parameters except Ψ_0 remained constant with $B=150000$, $m=4$, and $s=0.1$. Several values of Ψ_0 were tested in each method to find the most suitable value with which the density distribution calculated was the closest to that of the real proximal femur. After the trial, it was found that the most suitable value of Ψ_0 was 0.014 for the maximal cycle method and the stress maximum method, and 0.011 for the composite method. We chose 0.016 as a reference value to investigate the variation law from the results obtained. Three major volumes of interest (VOI) in proximal femur, i.e. femoral neck, greater trochanter, and ward's triangle, were chosen to compare the local density and L-T ratio.

As shown in Fig. 3, by using the maximal cycle method and the stress maximum method, the density calculated was much higher in ward's triangle than that in greater trochanter. Besides that, the transition between the two regions was extremely sharp. By using the composite method, the density distribution calculated corresponded well with the actual distribution in proximal femur. There was a wide high-density band from the upper edge of the femoral head to the lesser trochanter. The ward's triangle and the greater trochanter were low-density areas, and they were isolated by a narrow high-density band.

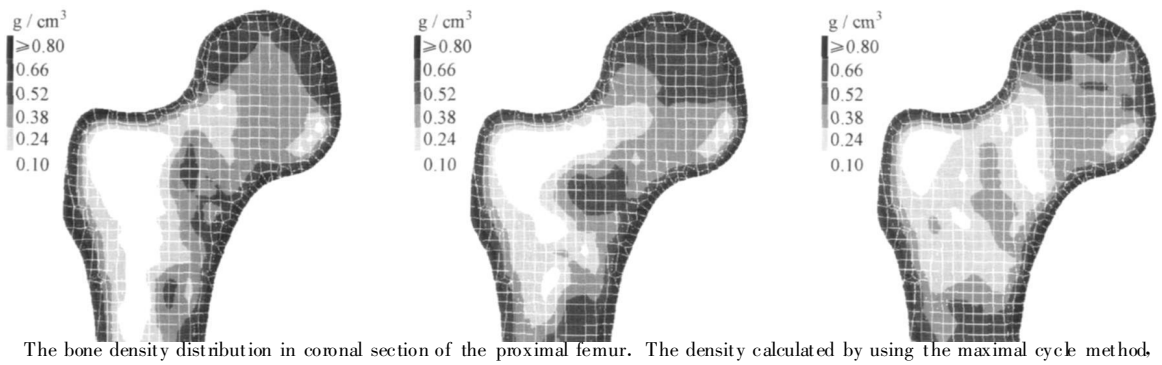

Fig. 3. The bone density distribution in coronal section of the proximal femur. The density calculated by using the maximal cycle method, the stress maximum method, and the composite method are shown from left to right.

The predicted trabecular alignments are displayed in Fig. 4. The arrows represent the projections of principal material axes in coronal section, which can denote the trabecula orientation. It can be seen

that the alignment of the trabeculae in the femoral head is irregular by using the stress maximum method, but it is regular by using the other two methods. By using the maximal cycle method, the most prominent trabeculae pointed to a single position, where the joint reaction force was applied to the femoral head in the first load case. In contrast, by using the composite method, the trabecula pointed to the nearest loading position belonging to any load case. Hence, all the loadings can affect the trabecular directions more or less according to the distance from the trabecula.

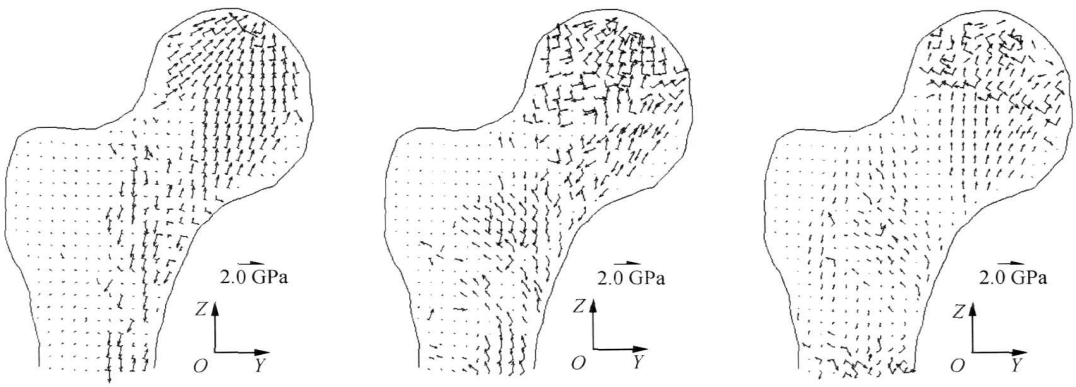

Fig. 4. The projections of principal material axes of trabecular bone in coronal section. The Young's moduli and material orientations derived from the maximal cycle method, the stress maximum method, and the composite method are been shown from left to right. The magnitude of arrow represents the Young's modulus.

The mean density in three local regions is illustrated in Fig. 5. It is obvious that the density decreases with the increasing equilibrium value. By using the maximal cycle method and the stress maximum method, the density obtained was almost equal in femur neck and ward's triangle for $\Psi_0 = 0.011$ and $\Psi_0 = 0.014$. The composite method has been shown to be the most stable one among the three methods because the characteristic remained the same for all the equilibrium values. The bone density was the highest in femur neck, and was more than twice that in the greater trochanter. It was a little higher in the ward's triangle than in the greater trochanter. These characteristics agreed with the actual observation by Martens et al. and Morgan et al.[23, 24].

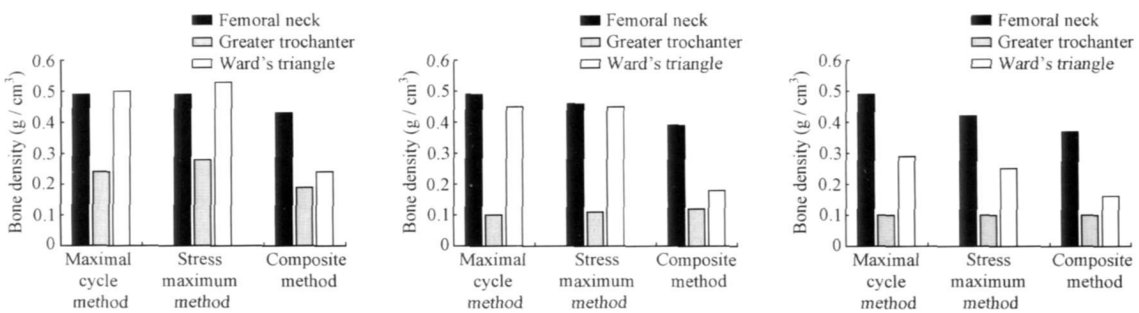

Fig. 5. The mean densities in three local regions. They were calculated by using the maximal cycle method, the stress maximum method, and the composite method, respectively. The equilibrium values used were 0.011, 0.014 and 0.016 from left to right.

The L-T ratio is shown in Fig. 6, and no obvious relationship can be found with the equilibrium value for all the methods. By using the stress maximum method, most L-T ratios were between 1.0 and 2.0, and the differences of L-T ratio among the three regions were the least. By using the maximal cycle method and composite method, the L-T ratio was significantly larger in femur neck than in the other two regions. This characteristic does not change with the equilibrium value.

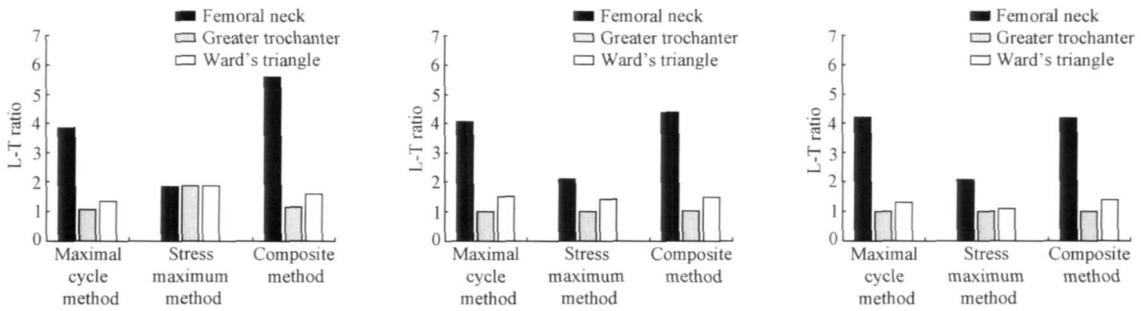

Fig. 6. The L-T ratios in three local regions. They were calculated by using the maximal cycle method, the stress maximum method, and the composite method, respectively. The equilibrium values used were 0.011, 0.014, and 0.016 from left to right.

3 Discussion

More and more evidence indicates that osteocytes can sense the mechanical stimulus and respond to it by activating the osteoblasts and osteoclasts. The osteoclasts are responsible for absorbing the bone matrix, leaving the lacuna in the bone surface. The osteoblasts fill the lacuna with new tissue[10, 25]. Due to the complicated biological mechanism involved in the bone remodeling, all the existing algorithms are based on some certain assumptions. Some researchers consider bone remodeling to be a self-regulating mechanism. The local bone formation or resorption is driven by the difference between the local mechanical stimulus and the equilibrium value in a certain location. This assumption can be modeled as the error driven algorithms, and the trabecular bone can be assumed to be either isotropic or orthotropic. It is reasonable that the growth of Young's modulus along a certain axis depends on the mechanical stimulus in this direction, and the trabecular bone is indeed orthotropic.

An orthotropic adaptation algorithm was utilized to simulate the remodeling process of the trabecular bone in this study. The key problem of this adaptation algorithm is the determination of orthotropic axes, which is not needed in isotropic algorithm. Naturally, the three principal stress directions should be chosen as the orthotropic axes under the single load case, since the trabecula aligns with the stress trajectory[25, 26]. However, it is difficult to determine the orthotropic axes under the multiple load cases because each load case corresponds to one group of the principal stress directions. Hence, some assumptions must be made on which each determination method is based. In the stress maximum method, it is assumed that only the single load case, under which the maximum of all the principal stresses is acquired, can determine the orthotropic axes. The other load cases have no effect on them. On the contrary, maximal cycle method is based on the assumption that only the load case with maximal cycles can determine the orthotropic axes. The common defect that the two methods share is that the local material axes of each element are only determined by the single load case. The composite method is based on the assumption that all the load cases contribute to the determination of orthotropic axes, and both loading cycles and principal stress are taken into consideration. The results had shown the validity of the three determination methods. For some elements nearer to each other, the predicted trabecular directions are likely to be determined by different single load cases according to the stress maximum method. So the trabecular directions are remarkably different though they are very near in distance, which leads to irregular distribution of trabecular alignment as a whole. With the maximal cycle method, the predicted directions of all elements are determined by the same load case, so most of the trabeculae point to one position. With the composite method, the trabecular directions are determined by all load cases for every element. So the distribution of trabecular alignment is regular and conforms to that of the real trabeculae shown by Martens et al.[23].

Three typical local regions were chosen to compare the validity of the three methods because density differences among different local regions depend on the adaptation algorithm. The drawbacks of the density distributions obtained by using the maximal cycle method and the stress maximum method are obvious. The density changes dramatically from the ward's triangle to the greater trochanter. In the ward's triangle, it is so high that it is almost equal to the density in the femur neck. With the composite method, the density in the ward's triangle and the greater trochanter is much lower than that in the femur neck. This characteristic is similar to that of the real femurs shown by Carter et al.[22].

There are also some limitations in this simulation. We assumed the outer shell of femur to be cortical bone, and the inner one to be trabecular bone. It was the same dividing method as that adopted by Miller et al.[17], and was not accurate enough to describe the real bone structure. Moreover, the load condition was simple. Only joint reaction force and abductor force were applied to the proximal femur, though this simplified consideration has been widely used in the past studies.

Orthotropic algorithm has many obvious advantages compared with the isotropic algorithm. The orientation characteristic can be displayed with it. The composite method has shown to be an effective method for determining the orthotropic axes. The orthotropic adaptation algorithm combining with real femur model plays a significant role in practical applications, such as the immobilization osteoporosis research.

References

1 Cowin SC. Bone stress adaptation models. ASME J Biomech Eng, 1993, 115(4B): 528—533

2 Baiotto S and Zidi M. Theoretical and numerical study of a bone remodeling model: The effect of osteocyte cells distribution. Biomechan Model Mechanobiol, 2004, 3(1): 6—16

3 Tsubota K and Adachi T. Spatial and temporal regulation of cancellous bone structure: Characterization of a rate equation of trabecular surface remodeling. Med Eng Phys, 2005, 27(4): 305—311

4 Turner CH. Three rules for bone adaptation to mechanical stimuli. Bone, 1998, 23(5): 399—407

5 Tezuka K, Wada Y and Takahashi A. Computer-simulated bone architecture in a single bone-remodeling model based on a reaction-diffusion system. J Bone Miner Metab, 2005, 23(1): 1—7

6 Subbarayan G and Bartel DL. A reconciliation of local and global models for bone remodeling through optimization theory. ASME J Biomech Eng, 2000, 122(1): 72—76

7 Schmitz MJ, Clift SE, Taylor WR, et al. Investigating the effect of remodelling signal type on the finite element based predictions of bone remodeling around the thrust plate prosthesis: a patient-specific comparison. Proc Inst Mech Eng Part H-J Eng Med, 2004, 218(6): 417—424

8 Huiskes R, Weinans H, Grootenboer HJ, et al. Adaptive bone-remodeling theory applied to prosthetic-design analysis. J Biomech, 1987, 20(11/12): 1135—1150

9 Beaupré GS, Orr TE and Carter DR. An approach for time dependent bone modeling and remodeling—theoretical development. J Orthop Res, 1990, 8(5): 651—661

10 Ruimerman R, van Rietbergen B, Hilbers PAJ, et al. A 3-dimensional computer model to simulate trabecular bone metabolism. Biorheology, 2003, 40(1—3): 315—320

11 Augat P, Link T, Lang TF, et al. Anisotropy of the elastic modulus of trabecular bone specimens from different anatomical locations. Med Eng Phys, 1998, 20(1): 124—131

12 Taylor WR, Roland E, Ploeg H, et al. Determination of orthotropic bone elastic constants using FEA and modal analysis. J Biomech, 2002, 35(6): 767—773

13 Yang G, Kabel J, Van Rietbergen B, et al. The anisotropic Hooke's law for cancellous bone and wood. J Elasticity, 1999, 53(2): 125—146

14 Wirtz DC, Schiffers N, Pandorf T, et al. Critical evaluation of known bone material properties to realize anisotropic FE-simulation of the proximal femur. J Biomech, 2000, 33(10): 1325—1330

15 Jacobs CR, Simo JC, Beaupré GS, et al. Adaptive bone remodeling incorporating simultaneous density and anisotropy considerations. J Biomech, 1997, 30(6): 603—613

16 Doblaré M and Garéa JM. Application of an anisotropic bone-remodelling model based on a damage-repair theory to analysis of the proximal femur before and after total hip replacement. J Biomech, 2001, 34(9): 1157—1170

17 Miller Z, Fuchs MB and Arcan M. Trabecular bone adaptation with an orthotropic material model. J Biomech, 2002, 35: 247—256

18 Watzky A and Naili S. Orthotropic bone remodeling: case of plane stresses. Mech Res Commun, 2004, 31(5): 617—625

19 Peng L, Bai J, Zeng X, et al. Comparison of isotropic and orthotropic material property assignments on femoral finite element models under two loading conditions. Med Eng Phys, 2006, 28(3): 227—233

20 Dong XN and Guo XE. The dependence of transversely isotropic elasticity of human femoral cortical bone on porosity. J Biomech, 2004, 37(8): 1281—1287

21 Keaveny TM and Hayes WC. A 20-year perspective on the mechanical properties of trabecular bone. ASME J Biomech Eng, 1993, 115(4B): 534—542

22 Carter DR, Fyhrie DP and Whalen RT. Trabecular bone density and loading history: Regulation of connective tissue biology by mechanical energy. J Biomech, 1987, 20(8): 785—794

23 Martens M, Van Audekercke R, Delport P, et al. The mechanical characteristics of cancellous bone at the upper femoral region. J Biomech, 1983, 16(12): 971—983

24 Morgan EF, Bayraktar HH and Keaveny TM. Trabecular bone modulus-density relationships depend on anatomic site. J Biomech, 2003, 36(8): 897—904

25 Huiskes R. If bone is the answer, then what is the question? J Anat, 2000, 197(2): 145—156

26 Turner CH, Anne V and Pidaparti RMV. A uniform strain criterion for trabecular bone adaptation: do continuum-level strain gradients drive adaptation? J Biomech, 1997, 30(6): 555—563